Friction **7**(3): 217–226 (2019)
https://doi.org/10.1007/s40544-018-0200-3
ISSN 2223-7690
CN 10-1237/TH
RESEARCH ARTICLE

Significant friction reduction of high-intensity pulsed ion beam irradiated WC-Ni against graphite under water lubrication

Gaolong ZHANG, Yuechang WANG, Ying LIU*, Xiangfeng LIU, Yuming WANG
State Key Laboratory of Tribology, Tsinghua University, Beijing 100084, China
Received: 09 July 2017 / Revised: 30 September 2017 / Accepted: 24 November 2017

Abstract: Two types of commercial WC-Ni samples were irradiated with the High-intensity pulsed ion beam (HIPIB). Both the surface characteristics and tribo-characteristics of the non-irradiated and irradiated WC-Ni samples, sliding against graphite under water lubrication, were compared. Quite low steady friction coefficients (approximately of 0.02) of the irradiated WC-Ni were observed. The surface topographies and components were investigated. The quite low friction of the irradiated WC-Ni samples was ascribed to the higher fluid retention capability of the latter and the tribofilm formed during sliding.

Keywords: WC-Ni; high-intensity-pulsed ion beam (HIPIB); low friction

1 Introduction

The Tungsten carbide (WC) based cemented carbides with metal binders, such as cobalt and nickel or binderless are widely utilized in cutting tools, mining machines and many tribological applications [1–7]. The wear resistance of the cemented carbide is significantly depended on the WC grain size, the porosity, the distribution, and the binder metal content, under various working conditions.

The wear resistance was different along the various crystallographic directions of a single crystal WC, as reported by Engqvist et al. [8], where the perpendicular prism was the best. Larsen-Basse [9] discovered that the high compression stress between the WC grains caused a binder plastic flow during sliding. This explained the quite higher binder content adjacently to the WC-Co sliding surface compared to the matrix body, whereas the lower content of the subsurface would cause a fracture. The appropriate WC size and binder content would improve the wear resistance of the cemented carbides [6, 10–12]. The wear debris, formed during dry sliding, would turn into the friction film, which could reduce friction; the higher *pv* (pressure × velocity) value would lead to a higher interface temperature and as a result the shear strengthening of the friction film decreased, contributing to a lower friction [13].

The corrosive and electrochemistry erosion effect of the lubricant had a high effect on the cemented carbide wear. The nickel binder had an improved wear resistance under the corrosive environment due to the Ni inert effect. A protective shell would be generated on the binder surface [14–17] and it would be preferable to be used under corrosive conditions. In contrast, the nickel binder mechanical strength was lower compared to the cobalt binder mechanical strength. In order to improve the mechanical strengthening of the WC-Ni, many reinforcement technologies have been invented by researchers [18–23]. The High intensity pulsed ion beam (HIPIB) irradiation has been proved to be an effective way to improve the mechanical strengthening, the hardness, and the wear resistance under dry conditions [19–23]. In contrast, the tribo-characteristics study of the HIPIB irradiated cemented carbide, working under a mixed lubrication, is limited. The requirement for the knowledge and applications of this technology

* Corresponding author: Ying LIU, E-mail: liuying@mail.tsinghua.edu.cn

increases due to industrial practices.

In the present work, two types of commercial WC-Ni samples with different nickel contents were irradiated with HIPIB. The tribo-tests of the non-irradiated and irradiated WC-Ni samples, sliding against resin impregnated graphite under water lubrication, were conducted. The topography, the tribological characteristics, and the surface components were compared. The friction reduction mechanism of the irradiated cemented carbides along with surface topography and the tribofilm were discussed.

2 Experimental procedure

2.1 Materials

Two types of commercial WC-Ni samples were utilized in the present work: (i) WC samples with 6%wt of Ni (YN6); (ii) WC samples with 10%wt of Ni (YN10). The average size of the WC grains was lower than 1 μm. The materials were converted into rings of 38 mm × 54 mm × 11 mm in dimensions. Commercial resin impregnated graphite rings of 41.5 mm × 50.5 mm × 5 mm in dimensions were utilized as the counter bodies in the tribo-tests. The working faces of the samples were lapped and polished with diamond slurry, consequently cleaned within an ultrasonic bath with ethanol and water, successively. All samples were supplied by the Ningbo Vulcan Mechanical Seals Manufacturing Co., Ltd., China.

2.2 HIPIB irradiation

The HIPIB irradiation on both the YN6 and YN10 samples was performed with the TEMP-6 HIPIB apparatus [24, 25]. As presented in Fig. 1(a), the sample was fixed on a movable platform, located within a vacuum chamber. Prior to irradiation, the platform was moved to a position which led the ion beam center to be located at the mean radius of the sample (Fig. 1(b)). In order to irradiate the entire surface of the sample, the platform was rotated 24° following a shot and 15 times in total for each sample. The ion beam of 40 mm in diameter was composed by 30% of proton and 70% of carbon ions. The acceleration voltage and ion current density were set at 200 kV and 80 A/cm^2, respectively (Fig. 1(c)). The real detected energy density was 2.5 J/cm^2.

2.3 Characterization

A light interferometer (Nexview, ZYGO, Middlefield, USA) was utilized to investigate the surface topographies of both non-irradiated and irradiated surfaces. The surface features and compositions were analyzed through scanning electron microscopy (SEM; Quanta 200 FEG, coupled with EDX) and X-ray photoelectron spectroscopy (XPS, PHI Quantera SXM, ULVAC-PHI, Japan).

2.4 Tribological tests

The ring-ring tribological tests were carried on under a deionized water lubrication condition. The inner and outer diameters of the friction area were 41.5 and 50.5 mm, respectively. Both the non-irradiated and irradiated WC-Ni rings were utilized as the stationary rings and the counter graphite rings rotated. The applied normal pressure and sliding speed were fixed at 0.72 MPa and 2.4 m/s according to the duty condition of the investigated thrust bearing. Each test lasted 2 hours. The wear rates of the WC-Ni samples were calculated through the worn surface profile. The

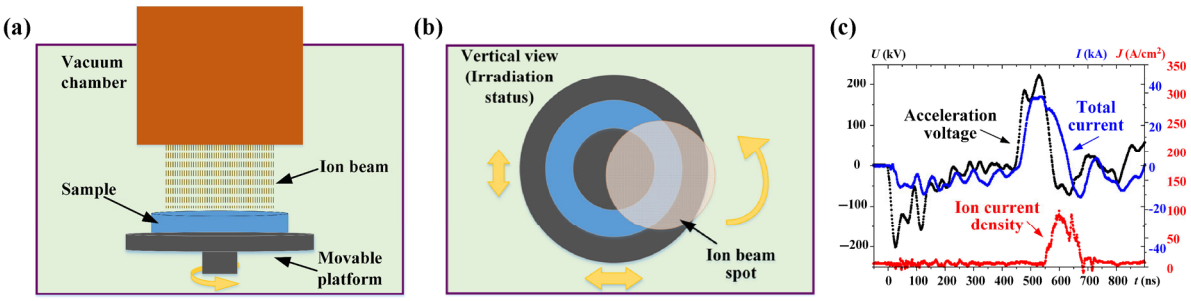

Fig. 1 (a) HIPIB irradiation schematic; (b) movable platform from vertical view; (c) irradiation status from vertical view; and (d) HIPIB parameters: acceleration voltage (black line), total current (blue), and ion current density (red).

schematic of the tribometer (PLINT TE92, Phoenix Tribology, UK) and the wear volumes determination are presented in Fig. 2. The detailed description of the tribo-meter could be found in the authors' previous work [26].

3 Results and discussion

3.1 Roughness and topography

The roughness of the non-irradiated/irradiated YN6 and YN10 surfaces were observed with the 3D white light interferometer, where each sample was measured by at least three positions of equidistance along the circumference. The non-irradiated WC-Ni surface was smooth with manufactured traces and pores (formed during sintering) upon it (Fig. 3(a)). In Fig. 3(b), the irradiated surfaces became rough and the hill/valley feature was marked.

The average Sa for the non-irradiated YN6 and YN10 surfaces was 10.7 nm and 13.3 nm, following the increased roughness of the irradiation samples to 30 nm for the YN6 and 32.5 nm for the YN10.

The SEM images of the non-irradiated and irradiated cemented carbides are presented in Fig. 4. Micro defects, such as pits and pores, existed among the grains and the binder, which were formed during sintering on the non-irradiated YN6/YN10 surface (Figs. 4(a) and 4(c)). Subsequently to irradiation (Figs. 4(b) and 4(d)), the manufacturing traces were removed and the pit edges became smooth. In contrast, holes and micro- cracks were also formed on the irradiated YN6/YN10 surfaces.

The HIPIB irradiation led to a high temperature on the shooting region. A melting and selective ablation would occur during irradiation [19–21]. As a result, the Ni content on the irradiated surface was lower. The WC grains on the surface sustained both the melting and re-solidification occurrences under the irradiation. These WC grains formed the hill/valley features, which increased the irradiated surface roughness. Both the thermal stress and stress concentration during fast heating and cooling might cause the micro-cracks generated on the irradiated surface [22].

Surface topographies have a high effect on the tribo-characteristics of the rubbing surfaces. Dong et al. [27] proposed three 3D functional parameters (surface bearing index S_{bi}, core fluid retention index S_{ci} and valley fluid retention index S_{vi}) to characterize the surface bearing property and the fluid retention ability, quantitatively. A higher surface bearing index indicates a good bearing property. Higher S_{ci} and S_{vi} indicates a good fluid retention property in the core zone and the valley zone, respectively.

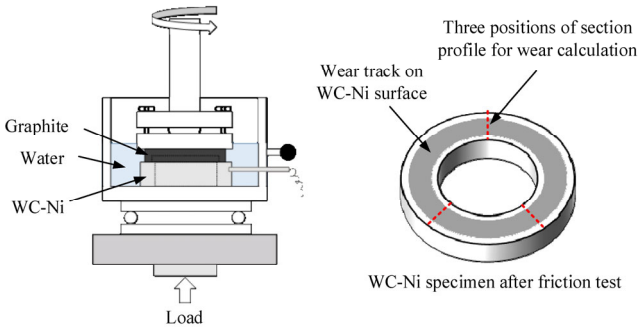

Fig. 2 Schematic of tribo-meter and the determination of wear volume.

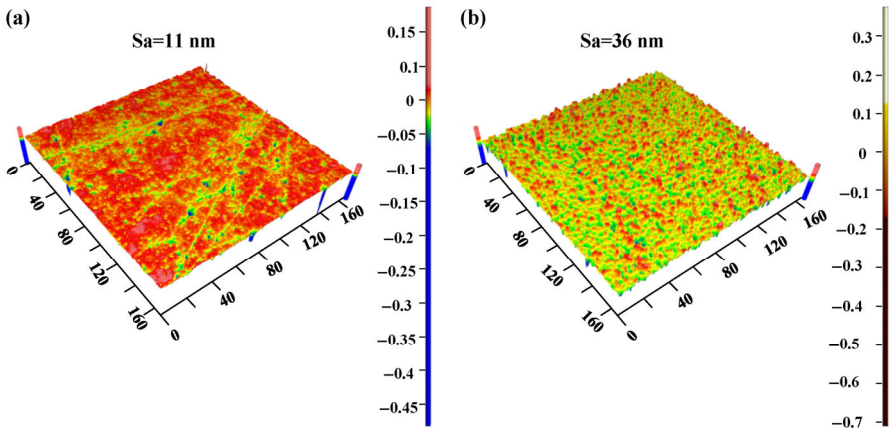

Fig. 3 Surface topographies of: (a) non-irradiated YN6; (b) irradiated YN6 (Unit: μm).

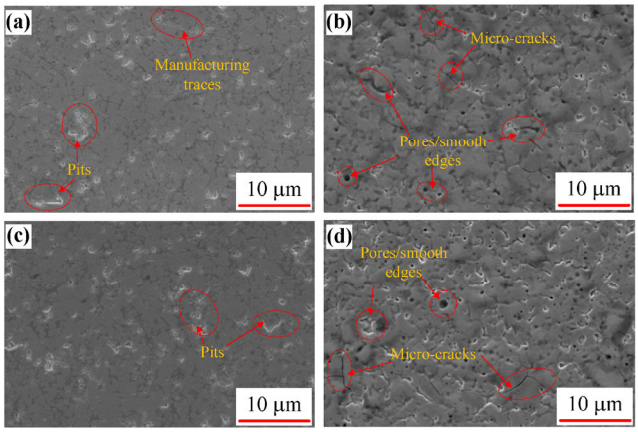

Fig. 4 WC-Ni SEM micrographs: (a) non-irradiated YN6; (b) irradiated YN6; (c) non-irradiated YN10; (d) irradiated YN10.

Figure 5 presents the S_{bi}, S_{ci}, and S_{vi} of the non-irradiated and irradiated surfaces. The values of S_{bi} of the non-irradiated surfaces were higher compared to the irradiated surfaces, because these non-irradiated lapping surfaces had a relatively flat surface (Fig. 4(a)). Following irradiation, the hills/valleys (Fig. 4(b)) formed on the surface led to the S_{bi} decrease. It meant that the non-irradiated surface had an improved bearing capacity compared to the irradiated surface. The core fluid retention index (S_{ci}) is characterized as the fluid retention property in the core zone of the surface. As presented in Fig. 5, the S_{ci} of the WC-Ni surfaces increased by irradiation. The irradiated surface had an improved fluid retention capacity in the core area of the surface. In mixed-lubrication condition, an increased amount of fluid could be reserved in the irradiated surface, which led the friction coefficient to decrease (Section 3.2). It should be noted that the valley fluid retention indexes (S_{vi}) are used to describe the fluid retention properties in the valley zones. These were slightly different between the non-irradiated and the irradiated surfaces. The friction behaviors of both the non-irradiated and irradiated surfaces were indifferent to the aforementioned indexes.

3.2 Friction

The friction coefficients of the non-irradiated and irradiated YN6/YN10 surfaces, sliding against graphite under deionized water are presented in Fig. 6. The steady friction coefficients of the non-irradiated YN6/YN10 sliding against graphite were of approximately 0.1; whereas the friction coefficients of the irradiated

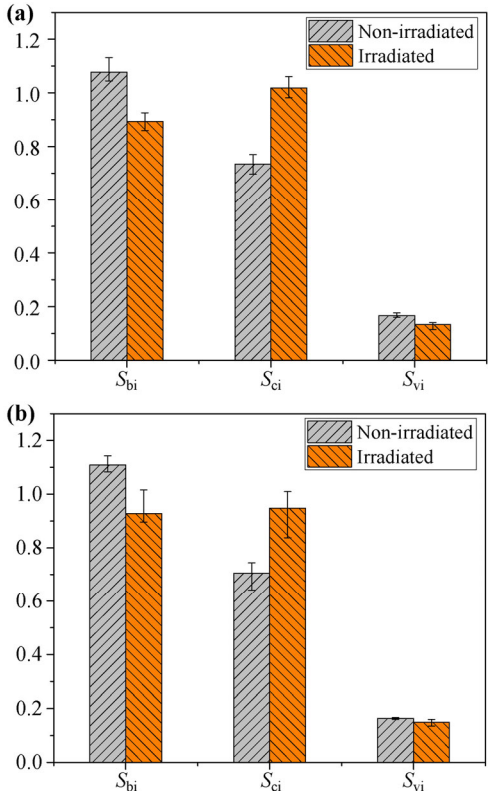

Fig. 5 Surface functional parameters of non-irradiated and irradiated cemented surfaces, (a) YN6; (b) YN10.

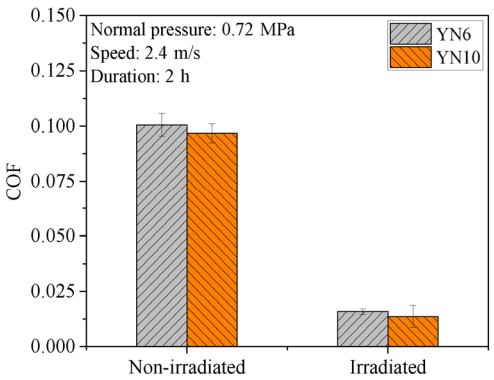

Fig. 6 Friction coefficient between graphite and non-irradiated/irradiated WC-Ni surface under water lubrication.

cemented carbides against graphite dropped dramatically and were below 0.02.

Both the SEM and EDX results of the cemented carbide and the graphite following the tribo-tests are presented in Fig. 7. The typical wear tracks along the sliding direction were observed on the non-irradiated cemented carbide worn surface (left of Fig. 7(a)) and "cloud" like features, comprising the C, W, Ni, and O were discovered on the counter graphite surface (right of Fig. 7(a)). These results were consistent with

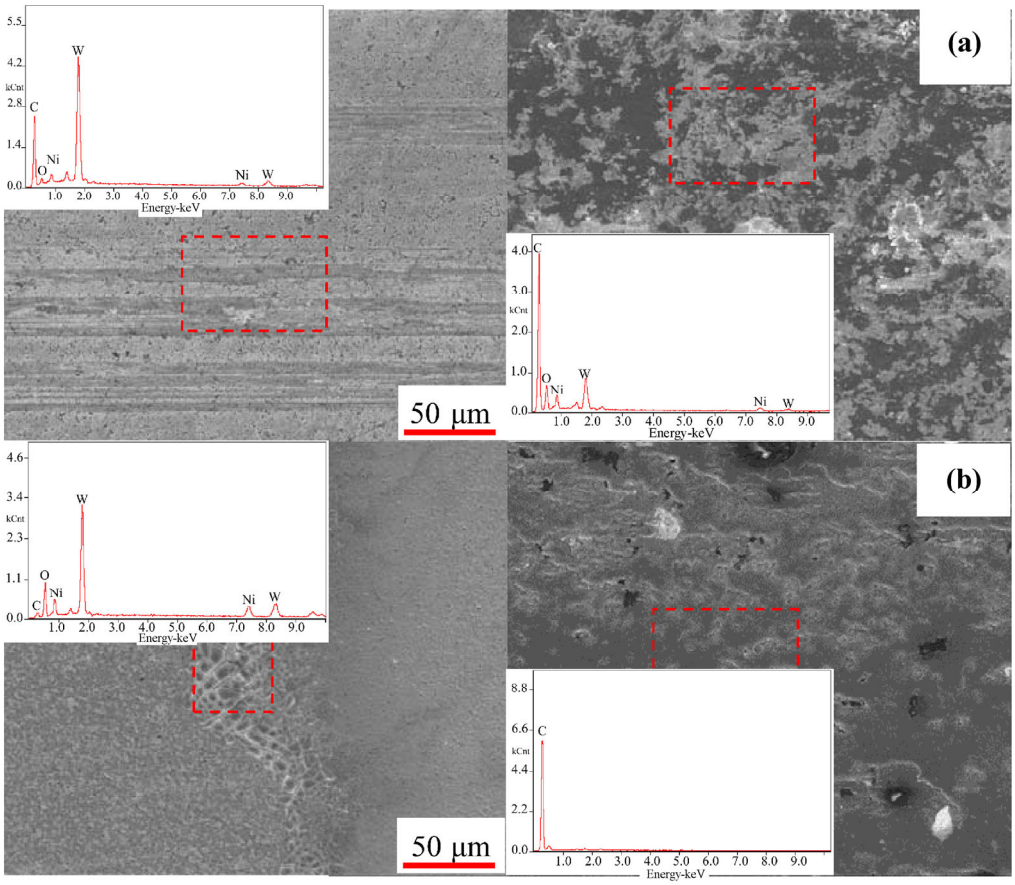

Fig. 7 SEM images of (a) non-irradiated YN6 (left) and counter graphite (right); (b) irradiated YN6 (left) and counter graphite (right). Insets were EDX spectra of marked regions.

the authors' previous reported results of the WC-Ni samples sliding against graphite under water lubrication [26]. Turtle shell-like features (left on Fig. 7(b)) were observed on the irradiated cemented carbide worn surfaces. The cloud like feature which was observed on graphite (Fig. 7(a), right) against the non-irradiated cemented carbide, while disappeared on these (Fig. 7(b), right) sliding against the irradiated cemented carbide.

The turtle shell region and the nearby regions were investigated further and the results are presented in Fig. 8. The EDX results demonstrated that the O content in region 2 was approximately of 69% (Fig. 8(c)), being significantly higher than the O content of the nearby regions (of 3.64% in region 1 and of 9.90% in region 3, Figs. 8(b) and 8(d)).

The friction coefficient of the friction pairs under a mixed lubrication could be described by Eq. (1).

$$f = r_s \times f_s + r_l \times f_l,\ r_s + r_l = 1 \tag{1}$$

where, f_s, f_l are the solid friction and liquid friction coefficients, respectively, and r_s, r_l are the ratios of the solid and liquid friction, respectively.

The reasons for the quite low friction of the irradiated surface could be clarified as follows. Firstly, the fluid retention ability in the core zone (S_{ci}) of the irradiated surface significantly increased (Fig. 5), which led to the r_l increase. Secondly, the tribo-film formed on the irradiated surface led to the reduction of the solid contact friction coefficient (f_s). Consequently, both the higher fluid contact ratio (r_l) and the lower solid contact friction coefficient contributed to the quite low friction coefficient of the irradiated WC-Ni sample, sliding against graphite under water lubrication.

3.3 Wear

Figure 9 demonstrates the wear volume of the non-irradiated and irradiated WC-Ni samples following the tribo-tests. The average wear volumes of the

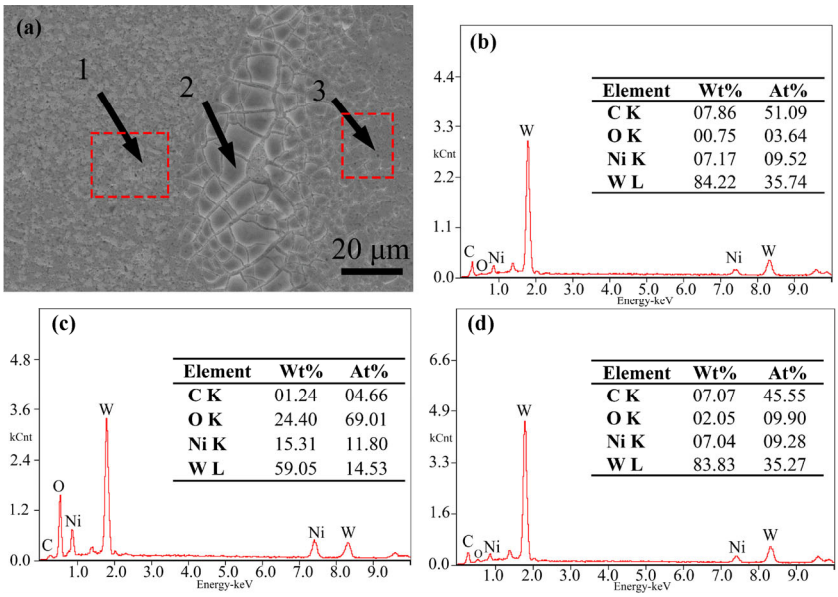

Fig. 8 Detailed investigation of irradiated YN6 surfaces following tribo-tests, (a) SEM image of irradiated YN6 surface following friction, (b)−(d) EDX spectrum of marked regions 1−3 in (a), respectively.

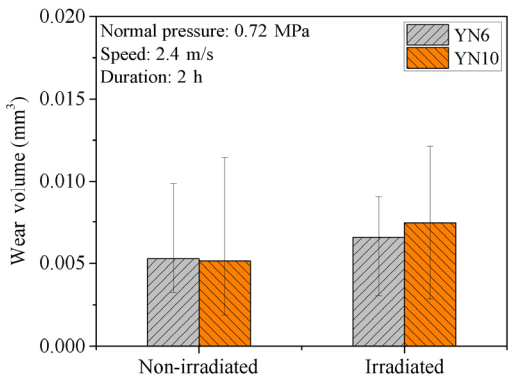

Fig. 9 Wear volume of non-irradiated/irradiated WC-Ni surfaces slid against graphite.

non-irradiated YN6 and YN10 surfaces were of approximately 5e-3 mm^3. Consequently, the average wear volumes of the irradiated YN6 and YN10 surfaces reached 6.6e-3 and 7.4e-3 mm^3, respectively. The wear volumes of the irradiated samples were higher compared to the non-irradiated samples.

In order to clarify the wear mechanism of both the non-irradiated and irradiated WC-Ni samples, the wear tracks of the non-irradiated/irradiated cemented carbides following sliding against graphite were also investigated through XPS. The W4f, C1s, O1s and Ni2p peaks were observed on the surface scan spectra (Figs. 10(a) and 11(a)). The Ni2p intensity on the non-irradiated WC-Ni worn surface was higher compared to the irradiated WC-Ni worn surface. The lower Ni intensity on the irradiated WC-Ni was also proved by the high resolution spectra of the Ni2p (Figs. 10(c) and 11(c)). The spectra of the W4f and O1s on the wear tracks of the non-irradiated and irradiated WC-Ni samples were quite different. On the non-irradiated WC-Ni wear track, the W could be ascribed to the WC (31.7) and WO_3 (34.5), whereas on the irradiated wear track the W was in the forms of WC (32) and WO_4^- (35.8). Only one O1s peak could be observed in the O high resolution spectrum on the wear track of the non-irradiated surface and this peak could be ascribed to the WO_3. Four O1s peaks could be observed on the wear track of the irradiated WC-Ni. These peaks corresponded to the O, which existed in the WO_3 (530.5), WO_4^- (531.3), $Ni(OH)_2$ (532.2) and H_2O (533.1). The XPS demonstrated that the constituents between the friction pairs of non-irradiated/graphite and irradiated/graphite were different. These differences were related to the tribo-behavior of both the non-irradiated and irradiated WC-Ni samples. As discussed in the authors' previous work, a transfer of WC and Ni into the graphite surface existed, whereas a cloudlike feature on the wear track of the graphite surface could be observed (right in Fig. 7(a)). For the irradiated WC-Ni, the tribo-chemistry of the irradiated surface was dominant and an apparent tribofilm

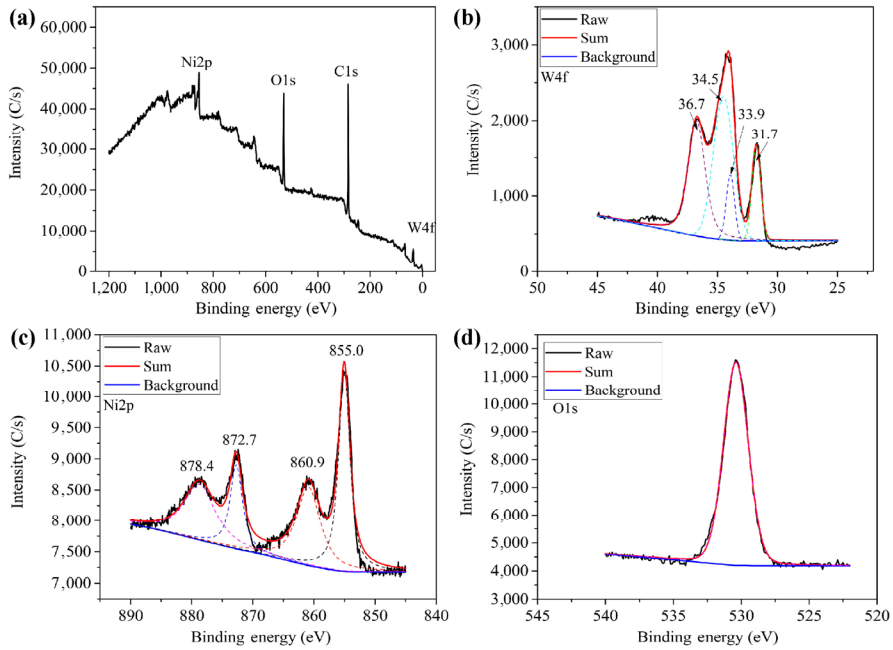

Fig. 10 XPS spectra of non-irradiated YN6 wear tracks: (a) surface scan; (b) W4f; (c) Ni2p; (d) O1s.

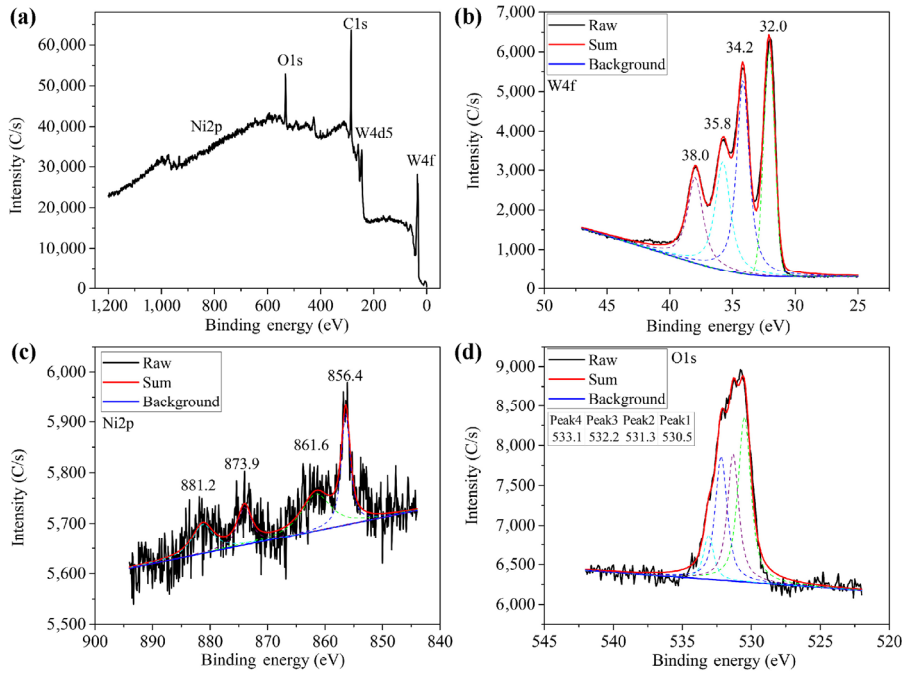

Fig. 11 XPS spectra of irradiated YN6 wear tracks: (a) surface scan; (b) W4f; (c) Ni2p; (d) O1s.

could be observed on the wear track of the irradiated surface (Fig. 7(b), left). It should be noted that all test samples were dried in the air. Consequently, the tribo-film was dried and cracked. This was possibly the reason for these turtle shell like features to be observed.

3.4 Friction and wear relationship

As aforementioned, the HIPIB irradiation could significantly reduce the friction coefficient of WC-Ni against graphite under water lubrication, however, the wear of the irradiated WC-Ni slightly increased.

This occurred because the non-irradiated and irradiated WC-Ni were governed by different wear regimes. The main wear mechanism of the non-irradiated WC-Ni samples sliding against graphite under water lubrication was micro-abrasion [28], while in the present work the irradiated WC-Ni wear was governed by tribo-chemistry.

Based on the SEM and XPS results, it could be inferred that the tribofilm, which was composed of the W and Ni (slight) oxidation, was generated during the tribo-tests of the irradiated WC-Ni samples against graphite under water lubrication. The tribo-film covered the asperities of the irradiated WC-Ni samples (Fig. 12(b)). The shear strength of the oxidation products was quite lower than the direct solid contact between the WC-Ni and the graphite asperities (Fig. 12(a)). As a consequence, a lower solid-solid friction was obtained, which made a significant contribution to the quite low friction of the irradiated WC-Ni.

During testing, a formation of tribo-film occurred and removed, reaching a balance at steady state. In contrast, the tribo-film was not protective, as evidenced by the turtle like features (Fig. 7(b) left, Fig. 8) on the wear trace of the irradiated WC-Ni samples. The irradiated WC-Ni sample wear consequently increased.

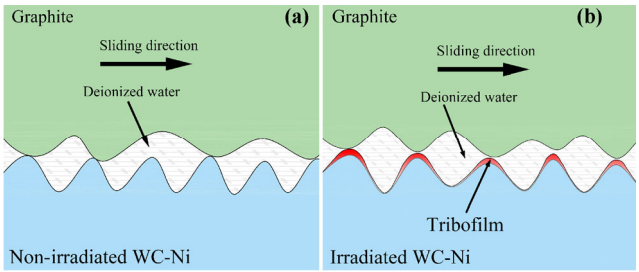

Fig. 12 Friction statures schematics of (a) non-irradiated WC-Ni; (b) irradiated WC-Ni against under deionized water.

4 Conclusions

In this study, two types of commercial cemented carbides with various Ni binder contents were modified through HIPIB irradiation. Both the corresponding surface topography and tribological characteristics during sliding against graphite under water lubrication were studied. It could be concluded that:

(1) The HIPIB irradiation could reduce the machining trace on the cemented carbide surfaces. In contrast, the surface roughness of the irradiated cemented carbides increased due to the selective ablation of Ni occurrence and the re-melting as well as the re-solidification of the WC grains.

(2) The core fluid retention capability of the cemented carbide surfaces increased subsequently to irradiation, leading to a lubrication effect increase under the mixed lubrication regime. The tribo-film, consisted of the oxidation products of W and Ni with low shearing resistance, contributing to the solid contact friction decrease. As a result, the quite low steady friction coefficient (lower than 0.02) was reached.

(3) The wear of the non-irradiated and irradiated WC-Ni samples, sliding against graphite under water lubrication, were governed by different regimes. The main wear mechanism of the non-irradiated WC-Ni samples was micro-abrasion, while the irradiated WC-Ni sample wear was governed by tribo-chemistry. Due to the low wear resistance of the tribo-film on the irradiated WC-Ni surface, the wear volume increased even though the friction coefficient was quite low.

Acknowledgements

The authors are grateful to the Key Lab of Materials Modification by Laser, Ion, and Electron Beams (Ministry of Education) for the HIPIB irradiation execution contribution and to Professor X. P. Zhu and M. K. Lei for their discussions and suggestions. This work was financially supported by both the National Basic Research Program of China (973) (Grant No. 2015CB057303) and the National Natural Science Foundation of China (Grant No. 51275268).

References

[1] Xie Y S, Jiang J J, Tufa K Y, Yick S. Wear resistance of materials used for slurry transport. *Wear* **332–333**: 1104–1110 (2015)

[2] Tsai K M, Hsieh C Y, Lu H H. Sintering of binderless tungsten carbide. *Ceram Int* **36**(2): 689–692 (2010)

[3] Kagnaya T, Boher C, Lambert L, Lazard M, Cutard T. Wear mechanisms of WC–Co cutting tools from high-speed tribological tests. *Wear* **267**(5–8): 890–897 (2009)

[4] Engqvist H, Botton G A, Ederyd S, Phaneuf M, Fondelius J, Axén N. Wear phenomena on WC-based face seal rings. *Int J Refract Met Hard Mater* **18**(1): 39–46 (2000)

[5] Engqvist H, Axén N, Hogmark S. Tribological properties of a binderless carbide. *Wear* **232**(2): 157–162 (1999)

[6] Cuddon A, Alien C. The wear of tungsten carbide-cobalt cemented carbides in a coal ash conditioner. *Wear* **153**(2): 375–385 (1992)

[7] Human A M, Northrop I T, Luyckx S B, James M N. A comparison between cemented carbides containing cobalt- and nickel-based binders. *J Hard Mater* **2**(3–4): 245–256 (1991)

[8] Engqvist H, Ederyd S, Axén N, Hogmark S. Grooving wear of single-crystal tungsten carbide. *Wear* **230**(2): 165–174 (1999)

[9] Larsen-Basse J. Binder extrusion in sliding wear of WC-Co alloys. *Wear* **105**(3): 247–256 (1985)

[10] Saito H, Iwabuchi A, Shimizu T. Effects of Co content and WC grain size on wear of WC cemented carbide. *Wear* **261**(2): 126–132 (2006)

[11] Van Acker K, Vanhoyweghen D, Persoons R, Vangrunderbeek J. Influence of tungsten carbide particle size and distribution on the wear resistance of laser clad WC/Ni coatings. *Wear* **258**(1–4): 194–202 (2005)

[12] Jia K, Fischer T E. Sliding wear of conventional and nanostructured cemented carbides. *Wear* **203–204**: 310–318 (1997)

[13] Engqvist H, Högberg H, Botton G A, Ederyd S, Axén N. Tribofilm formation on cemented carbides in dry sliding conformal contact. *Wear* **239**(2): 219–228 (2000)

[14] Engqvist H, Beste U, Axén N. The influence of pH on sliding wear of WC-based materials. *Int J Refract Met Hard Mater* **18**(2–3): 103–109 (2000)

[15] Human A M, Roebuck B, Exner H E. Electrochemical polarisation and corrosion behaviour of cobalt and Co(W,C) alloys in 1N sulphuric acid. *Mater Sci Eng A* **241**(1–2): 202–210 (1998)

[16] Human A M, Exner H E. The relationship between electrochemical behaviour and in-service corrosion of WC based cemented carbides. *Int J Refract Met Hard Mater* **15**(1–3): 65–71 (1997)

[17] Human A M, Exner H E. Electrochemical behaviour of tungsten-carbide hardmetals. *Mater Sci Eng A* **209**(1–2): 180–191 (1996)

[18] Guo H F, Tian Z J, Huang Y H, Yang H F. Microstructure and tribological properties of laser-remelted Ni-based WC coatings obtained by plasma spraying. *J Russ Laser Res* **36**(1): 48–58 (2015)

[19] Zhang F G, Zhu X P, Lei M K. Tribological behavior of WC-Ni cemented carbide irradiated by high-intensity pulsed ion beam. *Surf Coat Technol* **258**: 78–85 (2014)

[20] Zhu X P, Zhang F G, Song T K, Lei M K. Nonlinear wear response of WC-Ni cemented carbides irradiated by high-intensity pulsed ion beam. *J Tribol* **136**(1): 011603 (2014).

[21] Wen Q F, Liu Y, Wang Y M, Zhang F G, Zhu X P, Lei M K. The effect of irradiation parameters of high-intensity pulsed ion beam on tribology performance of YWN8 cemented carbides. *Surf Coat Technol* **209**: 143–150 (2012)

[22] Zhang F G, Zhu X P, Lei M K. Microstructural evolution and its correlation with hardening of WC-Ni cemented carbides irradiated by high-intensity pulsed ion beam. *Surf Coat Technol* **206**(19–20): 4146–4155 (2012)

[23] Zhang F G, Zhu X P, Wang M Y, Lei M K. Surface modification of WC-Ni cemented carbide for seals by high-intensity pulsed ion beam irradiation. *Acta Metall Sin* **47**(7): 958–964 (2011)

[24] Zhu X P, Lei M K, Ma T C. Characterization of a high-intensity bipolar-mode pulsed ion source for surface modification of materials. *Rev Sci Instrum* **73**(4): 1728–1733 (2002)

[25] Xin J P, Zhu X P, Lei M K. On time-of-flight ion energy deposition into a metal target by high-intensity pulsed ion beam generated in bipolar-pulse mode. *Surf Coat Technol* **206**(5): 879–883 (2011)

[26] Zhang G L, Liu Y, Guo F, Liu X F, Wang Y M. Friction characteristics of impregnated and non-impregnated graphite against cemented carbide under water lubrication. *J Mater Sci Technol* **33**(10): 1203–1209 (2017)

[27] Dong W P, Sullivan P J, Stout K J. Comprehensive study of parameters for characterising three-dimensional surface topography: III: Parameters for characterising amplitude and some functional properties. *Wear* **178**(1–2): 29–43 (1994)

[28] Zhang G L, Liu Y, Wang Y C, Guo F, Liu X F, Wang Y M. Wear behavior of WC-Ni sliding against graphite under water lubrication. *J Mater Sci Technol* **33**(11): 1346–1352 (2017)

Gaolong ZHANG. He received his master degree in mechanical engineering in 2013 from Beihang University, Beijing, China. He is a Ph.D. student in the Institute of Design Engineering (the Branch of the State Key Laboratory of Tribology) of Mechanical Engineering Department at Tsinghua University. His research interests include friction and wear of materials.

Ying LIU. She received her M.S. and Ph.D. degrees in mechanical engineering from Tsinghua University, China, in 1991 and 2003, respectively. She joined the Institute of Design Engineering (the Branch of the State Key Laboratory of Tribology) of Mechanical Engineering Department at Tsinghua University from 1991. Her current position is tenured Associate Professor. Her research interesting covers the design of mechanical seal system and study of water lubrication mechanism of bearing.